ENVIRONMENTAL RESEARCH
LETTERS

PURPOSE-LED PUBLISHING™
Celebrating the 20th anniversary of Environmental Research Letters

LETTER • **OPEN ACCESS**

A Southern moisture pathway accelerates wetting of the Tibetan Plateau

To cite this article: Fenying Cai and Xingwen Jiang 2026 *Environ. Res. Lett.* **21** 124015

View the article online for updates and enhancements.

You may also like

- Moisture source assessment and the varying characteristics for the Tibetan Plateau precipitation using TRMM
Chi Zhang
- Mechanisms of the decadal variability of monsoon rainfall in the southern Tibetan Plateau
Siyu Yue, Bin Wang, Kun Yang et al.
- Contrasting East Asian climate extremes in 2020 and 2022 tied to zonal flow
Chao He, Matthew Collins, Tianjun Zhou et al.

This content was downloaded from IP address 193.174.18.1 on 08/07/2026 at 12:33

ENVIRONMENTAL RESEARCH
LETTERS

Check for updates

OPEN ACCESS

RECEIVED
7 March 2026

REVISED
2 June 2026

ACCEPTED FOR PUBLICATION
8 June 2026

PUBLISHED
17 June 2026

Original content from this work may be used under the terms of the Creative Commons Attribution 4.0 licence.

Any further distribution of this work must maintain attribution to the author(s) and the title of the work, journal citation and DOI.

LETTER

A Southern moisture pathway accelerates wetting of the Tibetan Plateau

Fenying Cai[1,2] and **Xingwen Jiang**[3,4,*]

[1] Potsdam Institute for Climate Impact Research (PIK), Member of the Leibniz Association, PO Box 60 12 03, D-14412 Potsdam, Germany
[2] Department of Geography, Humboldt-Universität zu Berlin, 10099 Berlin, Germany
[3] Heavy Rain and Drought-Flood Disasters in Plateau and Basin Key Laboratory of Sichuan Province, Institute of Tibetan Plateau Meteorology, China Meteorological Administration, Chengdu, Sichuan 610072, People's Republic of China
[4] Institute of Tibetan Plateau Meteorology, Chinese Academy of Meteorological Sciences, Beijing 100081, People's Republic of China
[*] Author to whom any correspondence should be addressed.

E-mail: xingwen.jiang@yahoo.com

Keywords: Tibetan Plateau, complex networks, tropical-mid-latitude synergy, wetting trend

Supplementary material for this article is available online

Abstract

The Tibetan Plateau (TP), known as Asia's water tower, has experienced a pronounced wetting trend in recent decades, often attributed to moisture transport anomalies through western and eastern boundaries caused by westerly anomalies. Here we show that this explanation is incomplete. Using a complex network analysis, we find that humid air advection from the Atlantic is largely blocked by concurrent drying over the Iranian Plateau, precluding a western moisture supply. Instead, the TP wetting trend arises from intensified moisture inflow from the southern boundary. We identify a previously unrecognized mid-latitude wave train, triggered by European blocking, that enhances tropical moisture transport across the southern boundary of the TP. Over recent decades, the strengthening of this wave train, together with increased wetting over South Asia driven by asymmetric tropical Pacific warming, jointly amplifies TP hydrological changes. Our results reveal a synergistic coupling between tropical forcing and mid-latitude dynamics, providing a new framework for understanding the accelerated wetting of Asia's water tower.

1. Introduction

With an average elevation above 4000 m, the Tibetan Plateau (TP) is the largest concentrated area of glaciers outside the polar ice sheets (Immerzeel *et al* 2010, Bolch *et al* 2012, Yao *et al* 2022). Meltwater from its seasonal snowpack and numerous glaciers, serves as a vital water source for major rivers in Asia (Immerzeel *et al* 2010, Pritchard 2019, Li *et al* 2022). As a result, the water demand of almost 2 billion people in surrounding regions is influenced by the hydrological cycle of the TP, which is recognized as 'Asia's water tower' (Yao *et al* 2022). It is important to note that significant changes have been observed over the TP during the past decades, including glacier retreat (Yao *et al* 2012, 2022, Zhang *et al* 2023), lake expansion (Zhang *et al* 2017b, Li *et al* 2019a, Yao *et al* 2022, Li *et al* 2022), surface air moistening (Yang *et al* 2014, Zhang *et al* 2017c, Wang *et al* 2024), and north–south dipolar shifts in precipitation (Yao *et al* 2022, Jiang *et al* 2023a, Ding *et al* 2023, Luo *et al* 2025). Understanding these hydrological changes over the TP, a hotspot recognized as the 'Third Pole' of the Earth, is crucial for addressing global climate change.

Significant wetting trends over the TP have been observed simultaneously with drying trends over the Himalayas. These patterns also manifest as a north–south precipitation dipole. Some studies have attributed the precipitation and moisture changes to anthropogenic aerosol forcing (Jiang *et al* 2023a, Ding *et al* 2023, Wang *et al* 2024), while others have emphasized the role of internal variability in the climate system (Zhao *et al* 2022, Ding *et al* 2023). In particular, the uneven emission of anthropogenic aerosols weakened the Asian westerly jet, and then favored a dipolar precipitation trend over the TP (Wang *et al* 2024). In addition, the phase transition of the Interdecadal Pacific Oscillation induces an anomalous anticyclone over the northeastern TP, which weakens the westerlies on the east of TP and facilitates the convergence of

© 2026 The Author(s). Published by IOP Publishing Ltd

water vapor over the TP (Ding *et al* 2023). Specifically, the anomalous anticyclone over the northeastern TP is identified as part of a crucial teleconnection pattern influencing hydrological changes over the TP (Wang *et al* 2022, 2024, Ding *et al* 2023). However, our study identifies a previously unrecognized pathway characterized by an anomalous anticyclone over the southeastern TP, which bridges the mid-latitude and tropical signals and controls the atmospheric moisture budget of the TP.

The atmospheric moisture budget is critical for understanding the hydrological changes over the TP. It is directly regulated by local evaporation (Curio *et al* 2015, Zhao and Zhou 2021, Cheng *et al* 2024) and moisture transport through the TP's four boundaries (Zhang *et al* 2017a, He *et al* 2021). Climatologically, atmospheric water vapor over the TP primarily originates from its southern and western boundaries, with a larger input from the southern boundary (Feng and Zhou 2012, Li *et al* 2019b, Yan *et al* 2020). However, the variations and trends associated with four-boundary contributions remain a subject of considerable debate. A study using sensitivity simulations has revealed that the westerly jet stream modulates the seasonal cycle of the rainy season over the TP (Jiang *et al* 2023b). The interannual variations in rainfall and the water budget over certain regions of the TP are largely influenced by moisture transport from its western boundary rather than its southern boundary (Wang *et al* 2017b).

Using a Lagrangian particle dispersion model, a recent study attributes the decline in terrestrial water storage in the southern TP to trends in moisture carried by the westerlies from the Atlantic (Zhang *et al* 2023). Another study casts doubt on the contribution of the western upstream region, suggesting that a significant proportion of water vapor transported from the Atlantic may precipitate along the way and thus may not reach the TP (Zhao *et al* 2025). Meanwhile, several studies have focused on the weakened outflow through the eastern boundary due to anticyclonic circulation over the northeastern TP (Zhou *et al* 2019, Wang *et al* 2024). Such weakened outflow through the eastern boundary has been attributed to aerosol forcing over Eurasia, which partly explains the recent wetting over the TP. In addition, Indian Ocean warming has also been shown to contribute to this wetting (Zhou *et al* 2024). However, the potential interactions between tropical and mid-latitude changes relevant to recent TP wetting trends remain insufficiently understood and may have been underestimated.

In this study, we hypothesize that the mid-latitude westerlies may dynamically propagate wave signals, while the tropical monsoon thermodynamically supplies moisture. The synergistic effects between tropical and mid-latitude systems may contribute to the recent wetting trends over the TP. Specifically, we investigate the contributions of four boundaries associated with the occurrence of synoptic wet events over the TP, using complex climate network analysis and synoptic composite analysis with ERA5 reanalysis data (Hersbach *et al* 2020). Changes in moisture fluxes through the eastern and southern boundaries, induced by two distinct atmospheric wave trains, play a key role in the recent wetting trends over the TP. One of these wave trains has been well documented in previous studies (Wang *et al* 2017b, Wang *et al* 2024), whereas the other represents a synergistic westerly–monsoon modulation of the TP climate.

2. Methods

2.1. Datasets

Hourly air specific humidity (q), geopotential height, zonal wind, meridional wind, outgoing longwave radiation (OLR), surface pressure, and dew-point temperature at 2 m, are derived from the ERA5 reanalysis dataset (Hersbach *et al* 2020). These variables are averaged into daily and seasonal means, and are interpolated into 1° (lat) × 1° (lon) grid before further analysis. Near-surface specific humidity (q) is derived from dew-point temperature at 2 m. In addition, daily precipitation is derived from the dataset of CPC global unified gauge-based analysis of daily precipitation (Chen *et al* 2008). This study covers the summer season (June–July–August, JJA) for the period 1979–2023.

In addition, seasonal-mean 500-hPa specific humidity, zonal wind, and meridional wind from historical simulations of 39 climate models from the Coupled Model Intercomparison Project Phase 6 (CMIP6) during JJA for the period 1979–2014 (Eyring *et al* 2016), are analyzed in this study. The model outputs are interpolated into 1° × 1°. Thirty-nine models are adopted and one ensemble member is used for each model (see supplementary table S1).

2.2. Daily anomalous weather events

First, near-surface q and geopotential at 500 hPa (z500) are standardized. In the following, the 90th and 10th percentile thresholds are calculated from the standardized values during the whole 4140 d of the 45 summers during 1979–2023. At each grid cell, when the standardized anomaly of near-surface q exceeds its 90th threshold (drops below its 10th threshold), an anomalous atmospheric wet (dry) event is identified. Similarly, an anomalous high-pressure event at each grid point is recognized when standardized z500 is higher than its 90th threshold. This percentile-based criterion was chosen to retain a sufficient sample size while capturing representative anomalous conditions.

2.3. Complex network analysis

To investigate the significant concurrences between TP wet events, and large-scale anomalous weather events including wet, dry, and high-pressure events,

we construct three types of climate networks between: (1) TP wet events and Northern hemisphere (NH) wet events, (2) TP wet events and NH dry events, and (3) TP wet events and NH high-pressure events. For each pair of grid cells a and b, the link strength $L_{(a,b)}$ is determined by counting the total number of daily concurrences when an extreme event occurs over a and another happens over b simultaneously or with several-day lags, following previous studies (Cai *et al* 2024a, 2024b, 2026b). Specifically, the 0-, 2-, and 4-day lags are considered here, for three separate networks in each group. We use a maximum time lag of 4 days because a previous study based on composite analysis showed that high-pressure anomalies over Eastern Europe precede those over East Asia by 3–4 days (Cai *et al* 2024b). Notably, NH anomalous events precede the wet events over the TP, when considering time lags in the network analysis.

To identify the most robust connections in the networks, we retain only the top 5% of links ranked by link strength $L_{(a,b)}$ across all node pairs. In the following, for each type of anomalous weather event, we shuffle the time series of daily occurrences (absence as 0 or presence as 1) 1000 times, and then derive the 99th percentile threshold of the link strength $L_{(a,b)}$ from the 1000 shuffled values. Only when the observed $L_{(a,b)}$ exceeds the 99th percentile threshold, is this link identified as a significant one and will be retained. Otherwise, the nonsignificant link will be removed and the corresponding $L_{(a,b)}$ will be set to zero.

To clarify the signals linked to TP wet events explicitly, we calculate the cross-degree centrality inside TP wet events. It indicates the synoptic relevance of anomalous weather events with wet events occurring over the TP at synoptic scales. Degree centrality is the sum of significant link strengths to the grid cells belonging to the TP: $D_a = \sum_{b \in TP} L_{(a,b)}$, where wet events occur at grid cell b. The TP domain is defined as all grid cells with altitudes above 2500 m within 25°–45° N and 68°–110° E (see supplementary figure S1). To further illustrate the climate network analysis employed in this study, we provide a schematic diagram in supplementary figure S2.

2.4. Composite analysis

We further identify the TP regional wet events when large-scale wet events occur over the TP to characterize the detailed atmospheric circulation features. A day is recognized as a regional wet event, when anomalous wet events take place at no fewer than 93 grid cells of TP, following previous regional composite analyses (Cai *et al* 2024a, 2024b). The 90th percentile of the daily number of TP grid cells experiencing wet events corresponds to 93 grid cells. Therefore, based on the threshold of 93 grid cells, 419 d, approximately 10% of the total 4140 d, are identified as TP wet days. This criterion balances sample size with the selection of representative anomalous conditions.

The composite anomalies of TP regional wet events are calculated as the difference between the average over the 419 selected days and the climatology over the 4140 summer days. Before calculating the composite anomalies, the climatological mean is removed from all days to exclude the seasonal cycle. We further use Student's t-test to identify the statistical significance of the composite anomalies.

Moreover, we identify two distinct atmospheric teleconnection patterns: (1) Eastern Europe–Northeastern Tibetan Plateau (EE–NETP) pattern, and (2) Eastern Europe–Southeastern Tibetan Plateau (EE–SETP) pattern. An EE–NETP pattern is identified when both the daily z500 anomalies averaged over the EE (45°–65° N, 35°–60° E) and averaged over the NETP (38°–50° N, 96°–108° E) exceed the 80th percentile threshold. Similarly, an EE–SETP pattern is identified when both the daily z500 anomalies averaged over the EE and averaged over the SETP (22°–34° N, 92°–104° E) exceed the 80th percentile threshold. Specifically, 182 (265) days out of 4140 summer days are identified as EE–NETP (EE–SETP) patterns. The composite anomalies are calculated as the difference between the average for a given pattern and the climatology. Student's t-test is further used to identify the statistical significance level.

2.5. Pacific dipolar index

To investigate the influence of La Niña-like sea surface temperature (SST) trends, we calculate an interannual index to capture the asymmetric SST variations between the western and central-eastern equatorial Pacific. Specifically, the Pacific dipolar index is identified as the SST difference between the equatorial western Pacific (10° S–10° N, 120°–150° E) and central-eastern Pacific (5° S–5° N, 170°–120° W). The Pacific dipolar index is subsequently detrended and standardized.

3. Results

3.1. Hindering effect of the Iranian Plateau near the western boundary of the TP

We employ complex networks to reveal the large-scale characteristics of moisture transport over the TP and its surrounding regions. We hypothesize that pronounced water vapor transport is accompanied by atmospheric wet events that propagate continuously in space and time, which can be effectively captured using complex networks. Specifically, we examine the synoptic concurrence (i.e. nearly simultaneous occurrences; see supplementary figure S2) patterns of wet, dry, and high-pressure events, with wet events over the TP by analyzing the cross-degree centralities inside wet events over the TP (figure 1;

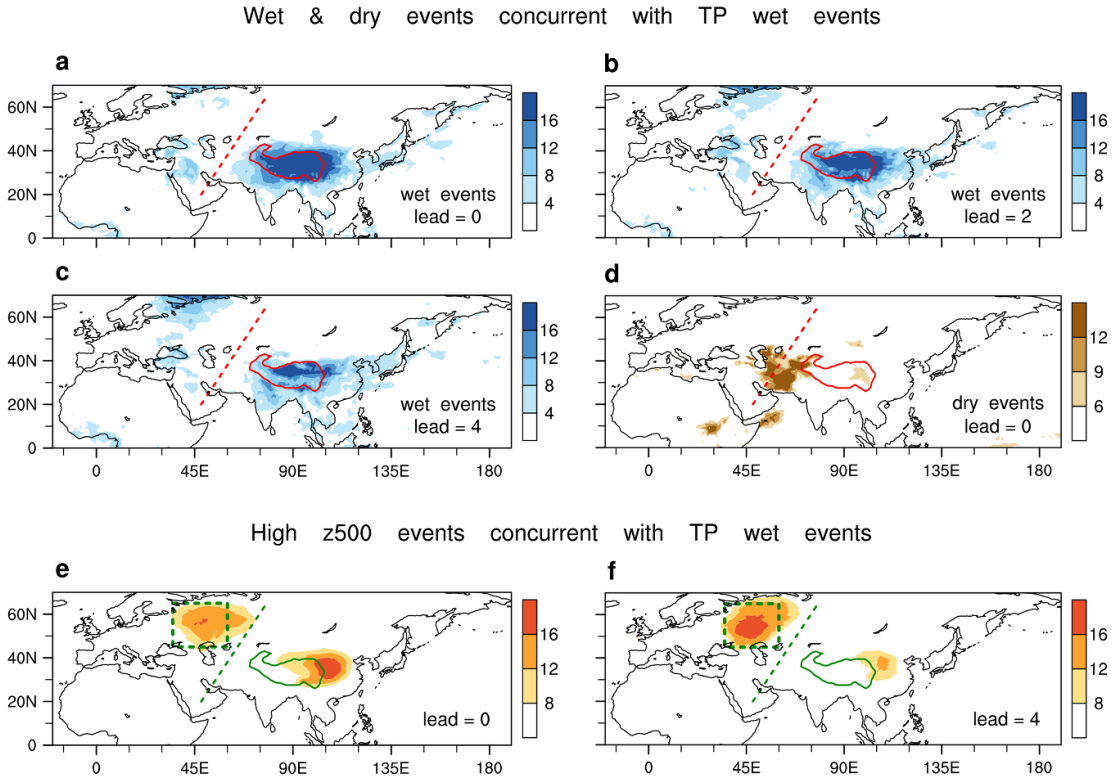

Figure 1. Dry events over the Iranian Plateau concurrent with wet events over the Tibetan Plateau (TP). Cross-degree centrality (units: ×1000) of Northern hemisphere wet events inside the TP wet events with a lag of (a) 0 day, (b) 2 days, and (c) 4 days. (d) Cross-degree centrality (units: ×1000) of Northern hemispheric dry events inside the TP wet events with no time lag. Cross-degree centrality (units: ×1000) of Northern hemisphere high-pressure events inside the TP wet events with a lag of (e) 0 day, (f) 4 days. For the lead-lag concurrences in (b), (c), and (f), the occurrences of the TP wet events are lagged. High values in (a)–(f) indicate high concurrences with the TP wet events. Colored contours in (a)–(f) outline the boundary of the TP with altitude of 2500 m inside the rectangular region (25°–45° N, 68°–110° E). The domains of Eastern Europe (45°–65° N, 35°–60° E) are indicated by green dashed boxes in (e), (f).

see Methods for details). Similar methods have been used to identify synoptic propagation and teleconnection patterns of extreme rainfall over South America (Boers *et al* 2014) and East Asia (Cai *et al* 2026a), extreme heatwaves over Eurasia (Jiang *et al* 2024, Cai *et al* 2024a, Wang *et al* 2025), and global impacts of El Niño (Fan *et al* 2017, Cai *et al* 2025).

In addition to local synchronization, wet events over the TP exhibit significant concurrences with wet events over South Asia, East Asia, Eastern Europe, and Turkey (figures 1(a)–(c)). There is clear evidence of moisture transport from the southern boundary of the TP, as wet events over South Asia typically occur 2–4 d ahead of those over the TP, characterized by a spatially continuous pattern (figures 1(b) and (c)). By contrast, upstream concurrences of wet events over Eastern Europe and Turkey are located more distantly, separated from wet events over the TP by the Iranian Plateau (figures 1(a)–(c)). Conversely, pronounced dry events over the Iranian Plateau occur simultaneously with wet events over the TP (figure 1(d)). This suggests that the simultaneous wet events over Eastern Europe and the TP are dynamically connected by an atmospheric Rossby wave, rather than by direct moisture transport. This is because their concurrences are discontinuous in space and are blocked by concurrent dry events over the Iranian Plateau (figure 1(d)). Our findings provide statistical evidence that is not entirely consistent with a previous study, which emphasized that a substantial amount of water vapor can be transported from the Atlantic to the TP (Zhang *et al* 2023). Rather, such moisture transport is hindered by dry events over the Iranian Plateau before reaching the western boundary of the TP (figure 1(d)).

To investigate the dynamical linkages between the upstream regions and the TP, we identify the concurrence patterns between large-scale anomalous 500-hPa high-pressure events and atmospheric wet events over the TP. We find that the TP wet events are strongly concurrent with high-pressure events over the eastern TP–East Asia (figures 1(e) and (f)). Such synoptic anticyclonic circulation anomalies increase surface specific humidity over the TP, the detailed mechanisms of which will be explained in the next section. Another notable concurrence of high-pressure events is observed over Eastern Europe, particularly during the 4 d preceding the wet events over the TP (figure 1(f)). These two high-pressure centers have been investigated as components of the Silk Road pattern (Wang *et al* 2017a, Wang *et al* 2023). These lead-lag concurrences at the synoptic time scale, are

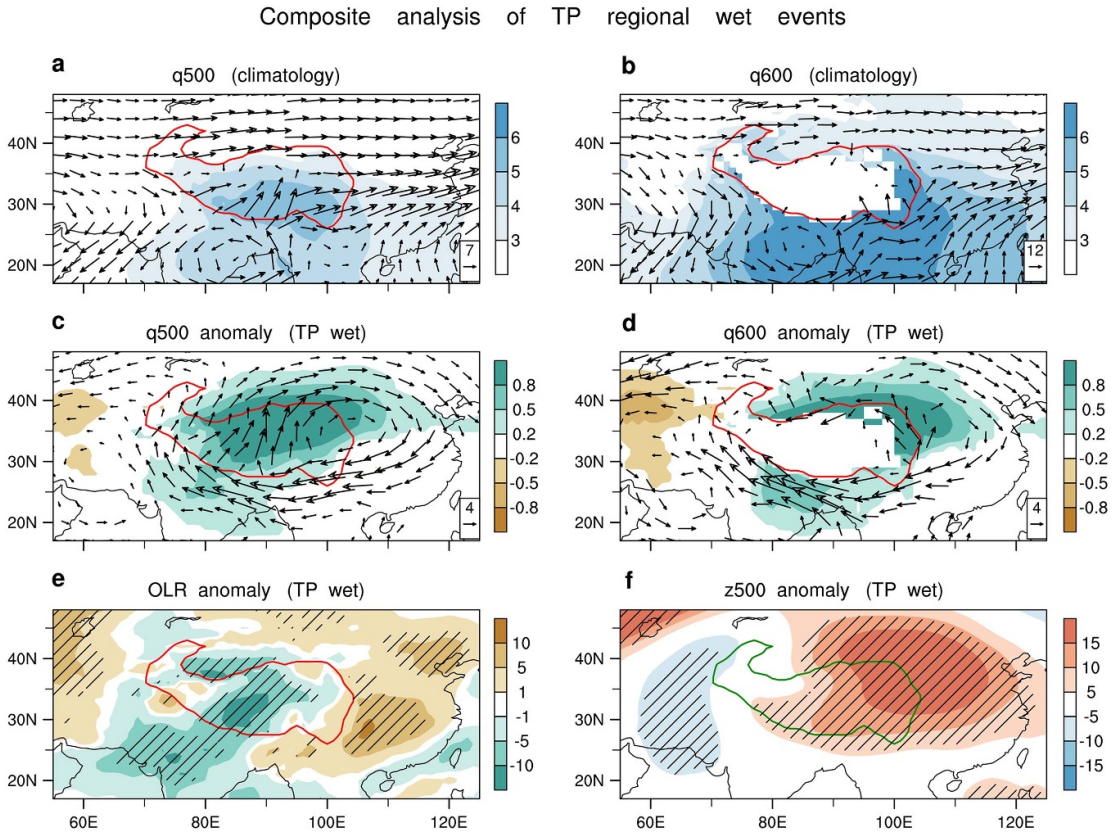

Figure 2. Occurrences of the Tibetan Plateau regional wet events attributable to anticyclonic circulation anomalies on its east. Climatology of specific humidity (shadings; units: g kg^{-1}), and moisture flux (vectors; units: g kg^{-1} m s^{-1}) (a) at 500 hPa, and (b) at 600 hPa. (c), (d) are the same as (a), (b), but for the composite anomalies, identified as the difference between the composite values of the TP regional wet events and the climatology. Composite anomalies of (e) outgoing longwave radiation (OLR; units: W m^{-2}), and (f) geopotential height at 500 hPa (z500; units: gpm). Colored contours in (a)–(f) outline the boundary of the TP with altitude of 2500 m inside (25°–45° N, 68°–110° E). Only significant anomalies ($p < 0.05$) are shown in (c), (d), and are hatched in (e), (f).

beneficial for predicting the occurrence of wet events over the TP.

3.2. Moisture transport linked to anticyclonic anomalies over the Eastern TP

In this section, we examine large-scale atmospheric circulation based on a composite analysis of TP regional wet events. Climatologically, moisture flow originates from the South Asian tropical monsoon region and the upstream mid-latitudes, converging to form a summertime high humidity center at 500 hPa over the southern TP (figure 2(a)). Previous studies have identified the southern and western boundaries as the major sources of atmospheric moisture over the TP (Feng and Zhou 2012, Li *et al* 2019b, Yan *et al* 2020). Accordingly, the moisture flow leaves the TP through its eastern boundary (figures 2(a) and (b)). During TP regional wet events, the high-humidity center at 500 hPa extends further northward, as a result of intensified moisture inflow from the southern boundary (figure 2(c)). By contrast, no significant increase in moisture input is observed through the western boundary (figures 2(c) and (d)). Meanwhile, easterly wind anomalies over the southeastern TP reduce the moisture outflow through the eastern boundary of the TP, leading to increased moisture accumulation over the Plateau (figures 2(c)–(d)). Therefore, the occurrence of wet events over the TP is attributable to anticyclonic circulation anomalies on its east (figure 2(f)). In addition, the composite analysis of TP regional wet events also reveals a significant negative anomaly of specific humidity at 500–600 hPa over the Iranian Plateau (figures 2(c) and (d)). This dry anomaly is linked to northeasterly wind anomalies associated with cyclonic circulation anomalies over the Iranian Plateau, which prevent the transport of humid air to the TP during its wet phases.

During the regional wet events, above-normal rainfall and enhanced convective activity are also observed over the TP, except in the southeastern part (figure 2(e); see supplementary figure S3(a)). Over the subsequent two days, regions with positive rainfall anomalies shift toward the northeastern TP, accompanied by a weakening of the high-pressure circulation anomalies to its east (see supplementary figures S3(c)–(f)).

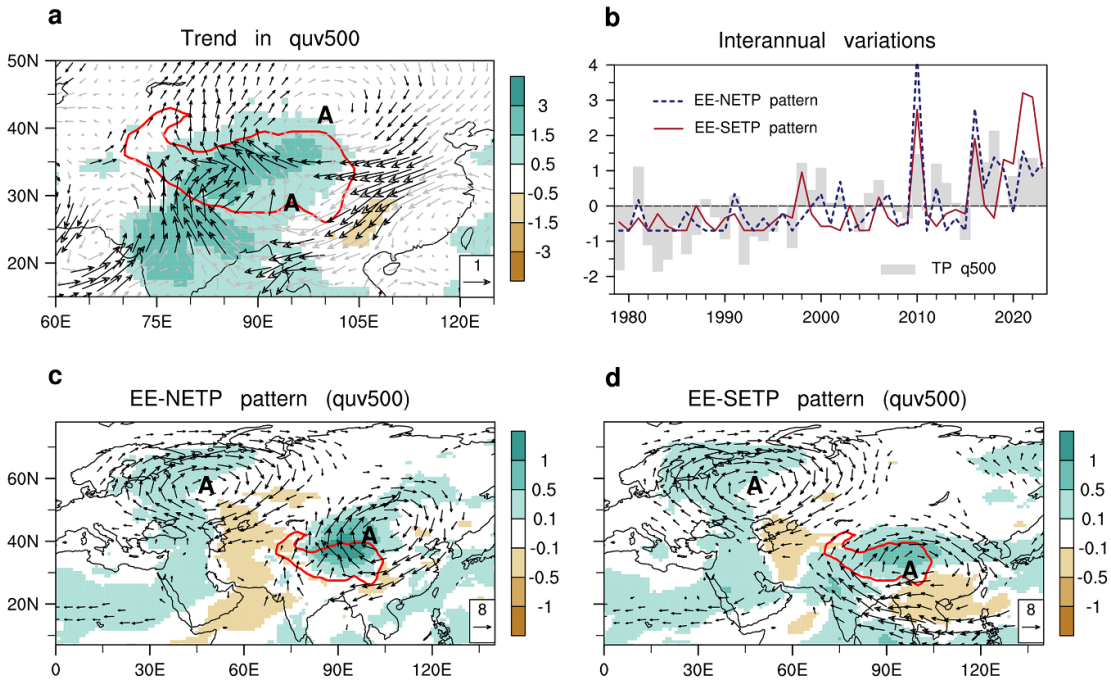

Figure 3. Two distinct atmospheric teleconnection patterns cause TP wetting. (a) Trends in 500-hPa specific humidity (shadings; units: 10^{-1} g kg^{-1} decade^{-1}; $p < 0.05$), and 500-hPa moisture flux (vectors; units: g kg^{-1} m s^{-1} decade^{-1}; $p < 0.05$). (b) Standardized time series of 500-hPa specific humidity averaged over the TP (gray bars), frequency of EE–NETP patterns (blue dashed line), and frequency of EE–SETP patterns (red solid line). Composite anomalies of specific humidity at 500 hPa (shadings; units: g kg^{-1}) and moisture flux at 500 hPa (vectors; units: g kg^{-1} m s^{-1}), for (c) EE–NETP pattern, and for (d) EE–SETP pattern. Only significant anomalies ($p < 0.05$ for shadings, and $p < 0.01$ for vectors) are plotted in (c), (d). Red contours in (a) and (c), (d) outline the boundary of the TP.

3.3. Synergistic influences of tropical and mid-latitude signals

Significant wetting trends are observed over the TP during the past four decades (figures 3(a) and (b)). To pinpoint the drivers of this wetting trend, we further examine the trends in 500-hPa moisture transport (figure 3(a)). Reduced outflow and enhanced inflow are observed through the eastern and southern boundaries of the TP, respectively (figure 3(a)), thereby causing the accumulation of atmospheric moisture over the TP. From the trends in vertically integrated moisture transport, the eastern boundary represents the dominant source, while the southern boundary also makes a substantial contribution to the wetting trend over the TP (see supplementary figure S4). Notably, the increasing trends in moisture transport through the eastern and southern boundaries correspond to two distinct anticyclonic circulation systems over the northeastern and southeastern TP, respectively (figure 3(a)). Network and composite analyses also indicate that high-pressure anomalies extend from the northeast to the southeast of the TP, appearing as two distinct centers (figures 1(e) and 2(f)). Therefore, we separate the atmospheric signals (see Methods for details) and find that the two distinct atmospheric teleconnection patterns regulate moisture transport through different boundaries of the TP (figures 3(c) and (d)).

The EE–NETP pattern manifests as two high-pressure anomalies over Eastern Europe and the northeast of the TP (figure 3(c)). This EE–NETP pattern reduces moisture outflow through the eastern boundary of the TP by inducing easterly wind anomalies (figure 3(c)). Such a mechanism has been illustrated in a previous study (Wang *et al* 2024). By modulating the moisture transport through the eastern boundary, aerosol forcing have contributed to the wetting trends over the TP in recent decades (Wang *et al* 2024).

However, this study focuses on the other atmospheric teleconnection pattern, i.e. the EE–SETP pattern, because it is less well understood than the EE–NETP pattern. Specifically, apart from the high-pressure anomaly over Eastern Europe, a second high-pressure anomaly is observed over the southeastern TP (figure 3(d)). During the EE–SETP pattern, wave energy is less likely to propagate toward northern China, likely owing to the absence of a strong meridional potential-vorticity gradient (see supplementary figures S5(a)–(d)), which acts as a waveguide associated with an intensified jet stream (Xie *et al* 2023, 2025). Moreover, suppressed convection over the South China Sea and the Indochinese Peninsula is observed during the EE–SETP pattern (see supplementary figure S5(f)), but not during the EE–NETP pattern (see supplementary figure S5(e)). This

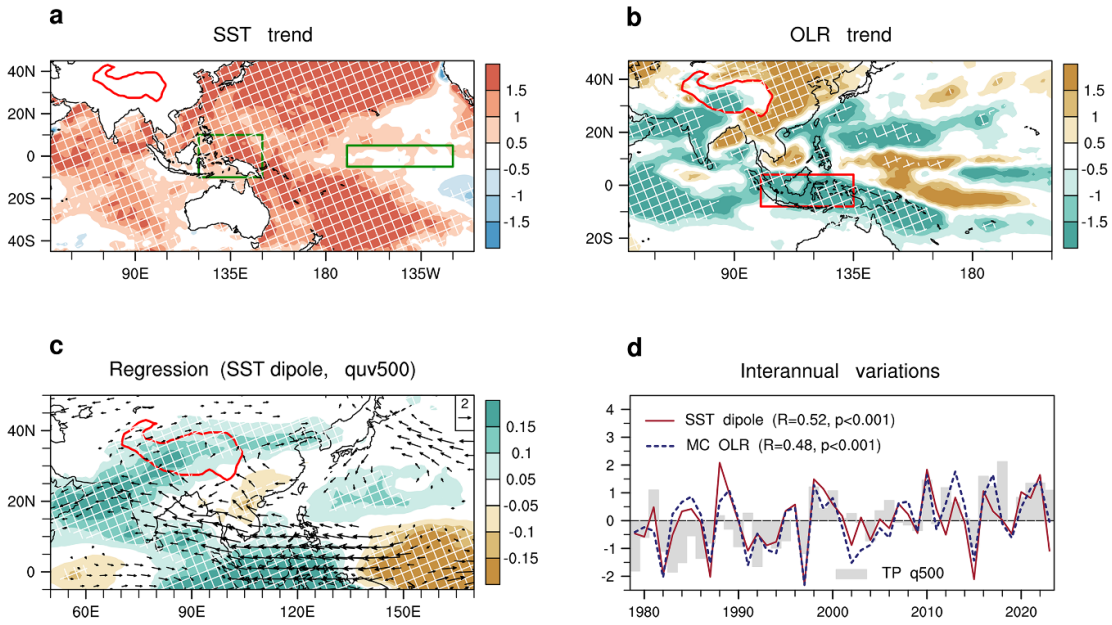

Figure 4. Contributions of tropical sea surface temperature (SST) and convection patterns. Temporal trends in (a) SST (units: 10^{-1} K decade^{-1}), and in (b) outgoing longwave radiation (OLR; units: W m^{-2} decade^{-1}). (c) Regression coefficients of specific humidity at 500 hPa (shadings; units: g kg^{-1}) and moisture transport at 500 hPa (vectors; units: g kg^{-1} m s^{-1}) onto the standardized time series of Pacific dipolar index. (d) Standardized time series of 500-hPa specific humidity averaged over the TP (gray bars), convection over the Maritime Continent (blue dashed line), and the Pacific dipolar index (red solid line). Red contours in (a)–(c) outline the boundary of the TP. Green boxes in (a) indicate the regions for identifying the Pacific dipolar index. Red box in (b) outlines the domain of the Maritime Continent (8° S–4° N, 100°–135° E). Significant trends and anomalies ($p < 0.05$) are cross-hatched in (a)–(c).

contrast may partly explain the difference between the two patterns, as anomalous convection can intensify anticyclonic circulation over the southeastern TP through a Rossby wave response.

The EE–SETP pattern transports humid air from South Asia to the TP via enhanced northward moisture advection through the southern boundary of the TP (figure 3(d)). Tropical convective storms over India can lift moisture into the mid-troposphere, from where it is subsequently transported to the TP (Dong *et al* 2016). This indicates a synergistic effect in which the mid-latitude westerlies dynamically propagate wave signals, while the tropics supply moisture. It is highlighted in this study that the TP wetting trends are also driven by enhanced moisture input from the southern tropics, which is distinguished from the well-recognized impacts of anthropogenic aerosols on the mid-latitude circulation. Increased mid-tropospheric atmospheric moisture over the tropical South Asia acts as an important source (Dong *et al* 2016) and may accelerate the wetting trend over the TP (figure 3(a)).

During both wave-train events, westward extension of the western North Pacific Subtropical High coincides with an intensified and eastward-expanded South Asian High (see supplementary figure S6). These changes favor enhanced moisture transport to the TP through dynamic and thermodynamic processes (Jiang *et al* 2025). Nevertheless, the two wave patterns show a detrended interannual correlation of 0.59, possibly because both originate over Eastern Europe. Yet this relationship explains only ∼35% of the variance, highlighting the need to disentangle their respective influences. Significant intensifications of both distinct patterns favor wetting trends over the TP (figure 3(b)). It is important to note that multiple CMIP6 models fail to reproduce the trends of the two separate anticyclonic centers over the eastern TP and the two distinct moisture transport pathways, even in models that simulate the strongest wetting trends over the TP (see supplementary figure S7), raising concerns about the reliability of studies based on CMIP6 simulations.

Furthermore, South Asia has become wetter over the past decades (figure 3(a)). This tropical change may accelerate the wetting trends over the TP, as the tropics act as an important moisture source for the TP. Our analysis suggests that the asymmetric trends in the tropical Pacific SST play a key role (figure 4). Faster warming has been observed in the tropical western Pacific than the central-eastern Pacific, exhibiting La Niña-like SST trends (figure 4(a)). This tropical Pacific asymmetric warming has led to a pronounced intensification of convection over the Maritime Continent (figure 4(b)). The easterly anomalies associated with intensified convection over the Maritime Continent transport moisture toward South Asia (figure 4(c)). As a result, wetting trends

over South Asia, as well as those over the TP, are driven by asymmetric SST trends in tropical Pacific (figure 4).

4. Conclusions and discussions

Our study investigates the specific contributions of moisture transport through the four boundaries of the TP, relevant to its recent wetting trends. During the wet events occurring over the TP, humid air from the Atlantic is hindered by concurrent dry events over the Iranian Plateau, before moisture carried by westerly winds reaches the western boundary of TP. Rather, reduced outflow through the eastern boundary as well as enhanced inflow through the southern boundary are crucial for the moisture accumulation over the TP. We specifically find that two distinct atmospheric teleconnection patterns modulate these moisture transports through the eastern and southern boundaries, respectively. It is noteworthy that the wave trains propagating toward the southeastern TP are less well understood than those toward the northeastern TP. This southeastward-propagating wave train bridges signals between the tropics and the mid-latitudes. Specifically, the mid-latitude westerlies dynamically propagate wave signals, while the tropics supply moisture. Intensifications of both the mid-latitude wave trains and wetting trends over South Asia caused by asymmetric ocean warming in the tropical Pacific, jointly contribute to recent wetting trends over the TP.

We find that tropical convection over India is closely linked to the EE–SETP pattern on synoptic timescales and in long-term trends. However, the complex interplay between tropical convection and mid-latitude wave trains is not discussed in depth in this study and deserves further investigation using well-designed model experiments. In addition, this study is limited to a historical analysis of wetting trends over the TP. Substantial biases remain in the simulation of the underlying mechanisms, particularly the westerly–monsoon synergy driving the TP wetting trends emphasized in this study. Nevertheless, the historical analysis presented here provides valuable implications for improving future climate projections.

Acknowledgments

X J is supported by the National Key Research and Development Program of China (2023YFC3007501), Sichuan Science and Technology Program(No.2025YFNH0006); Major science and technology project of the Xizang Autonomous Region (XZ202402ZD0006), the National Natural Science Foundation of China (42075045), the Youth Innovation Team of China Meteorological Administration 'Climate change and its impacts in the Tibetan Plateau' (CMA2023QN16). F C acknowledges the support and scholarship from the China Scholarship Council (CSC).

Data availability statement

The ERA5 single-level and multi-level variables are available at https://doi.org/10.24381/cds.adbb2d47 and https://doi.org/10.24381/cds.bd0915c6, respectively (Hersbach *et al* 2020). CPC precipitation dataset (Chen *et al* 2008) could be freely derived from https://psl.noaa.gov/data/gridded/data.cpc.globalprecip.html. The outputs of CMIP6 simulations (Eyring *et al* 2016) are freely downloaded from https://esgf-node.llnl.gov/search/cmip6/. The codes used to generate the figures in this study are available on request from the authors.

All data that support the findings of this study are included within the article (and any supplementary files).

Supplementary data 1 available at https://doi.org/10.1088/1748-9326/ae798d/data1.

Author contributions

Fenying Cai 0009-0004-0572-4179
Conceptualization (equal), Data curation (equal), Formal analysis (lead), Investigation (equal), Methodology (lead), Resources (equal), Software (equal), Validation (equal), Visualization (equal), Writing – original draft (lead)

Xingwen Jiang
Conceptualization (equal), Formal analysis (equal), Funding acquisition (lead), Investigation (lead), Project administration (lead), Supervision (lead), Writing – review & editing (lead)

References

Boers N, Bookhagen B, Barbosa H M, Marwan N, Kurths J and Marengo J A 2014 Prediction of extreme floods in the eastern central Andes based on a complex networks approach *Nat. Commun.* **5** 5199

Bolch T *et al* 2012 The state and fate of Himalayan glaciers *Science* **336** 310–4

Cai F, Gerten D, Zhang K, Zhang T, Yang S and Kurths J 2026b Large-scale aggregation of humid heatwaves exacerbated by coastal oceanic warming *Nat. Geosci.* **19** 513–9

Cai F, Lin S, Gerten D, Yang S, Jiang X, Su Z and Kurths J 2025 Intensified dominance of El Niño-like convection relevant for global atmospheric circulation variations *npj Clim. Atmos. Sci.* **8** 242

Cai F, Liu C, Gerten D, Yang S, Zhang T, Li K and Kurths J 2024a Sketching the spatial disparities in heatwave trends by changing atmospheric teleconnections in the Northern hemisphere *Nat. Commun.* **15** 8012

Cai F, Liu C-H, Yang S, Deng K-Q and Kurths J 2024b Linkage between European and East Asian heatwaves on synoptic scales *J. Trop. Meteorol.* **30** 97–105
Cai L, Yuan N, Boers N and Kurths J 2026a Global teleconnections of extreme rainfall events in the Yellow River basin *Adv. Atmos. Sci.* **43** 933–48
Chen M *et al* 2008 Assessing objective techniques for gauge-based analyses of global daily precipitation *J. Geophys. Res.* **113** D04110
Cheng T F, Chen D, Wang B, Ou T and Lu M 2024 Human-induced warming accelerates local evapotranspiration and precipitation recycling over the Tibetan Plateau *Commun. Earth Environ.* **5** 388
Curio J, Maussion F and Scherer D 2015 A 12-year high-resolution climatology of atmospheric water transport over the Tibetan Plateau *Earth Syst. Dyn.* **6** 109–24
Ding Z, Zhai P and Wu R 2023 Recent change in summer rainfall over the Tibetan Plateau: roles of anthropogenic forcing and internal variability *Clim. Dyn.* **61** 1887–902
Dong W *et al* 2016 Summer rainfall over the southwestern Tibetan Plateau controlled by deep convection over the Indian subcontinent *Nat. Commun.* **7** 10925
Eyring V, Bony S, Meehl G A, Senior C A, Stevens B, Stouffer R J and Taylor K E 2016 Overview of the coupled model intercomparison project phase 6 (CMIP6) experimental design and organization *Geosci. Model Dev.* **9** 1937–58
Fan J, Meng J, Ashkenazy Y, Havlin S and Schellnhuber H J 2017 Network analysis reveals strongly localized impacts of El Niño *Proc. Natl Acad. Sci. USA* **114** 7543–8
Feng L and Zhou T 2012 Water vapor transport for summer precipitation over the Tibetan Plateau: multidata set analysis *J. Geophys. Res.* **117** D20114
He Y, Tian W, Huang J, Wang G, Ren Y, Yan H, Yu H, Guan X and Hu H 2021 The mechanism of increasing summer water vapor over the Tibetan Plateau *J. Geophys. Res.* **126** e2020JD034166
Hersbach H *et al* 2020 The ERA5 global reanalysis *Q. J. R. Meteorol. Soc.* **146** 1999–2049
Immerzeel W W, van Bee L P H and Bierkens M F P 2010 Climate change will affect the Asian water towers *Science* **328** 1382–5
Jiang J, Liu Y, Meng J, Wu G, He B, Ma T, Bao W and Fan J 2024 Dry soil moisture on the Tibetan plateau drives synchronous extreme heatwaves in Europe and East Asia *npj Clim. Atmos. Sci.* **7** 281
Jiang J, Zhou T, Qian Y, Li C, Song F, Li H, Chen X, Zhang W and Chen Z 2023a Precipitation regime changes in high Mountain Asia driven by cleaner air *Nature* **623** 544–9
Jiang R, Jiang X, Li L and Lu P 2025 Rapid increase in extreme hourly precipitation in recent two decades in the Tibetan Plateau and its large-scale drivers *Geophys. Res. Lett.* **52** e2025GL117722
Jiang X, Cai F, Li Z, Wang Z and Zhang T 2023b The westerly winds control the zonal migration of rainy season over the Tibetan Plateau *Commun. Earth Environ.* **4** 363
Li X, Long D, Scanlon B R, Mann M E, Li X, Tian F, Sun Z and Wang G 2022 Climate change threatens terrestrial water storage over the Tibetan Plateau *Nat. Clim. Change* **12** 801–7
Li X, Long D, Huang Q, Han P, Zhao F and Wada Y 2019a High-temporal-resolution water level and storage change data sets for lakes on the Tibetan Plateau during 2000–2017 *Earth Syst. Sci. Data* **11** 1603–27
Li Y, Su F G, Chen D L and Tang Q H 2019b Atmospheric water transport to the endorheic Tibetan Plateau and its effect on the hydrological status in the region *J. Geophys. Res.* **124** 12864–81
Luo H, Chen D, Yang S, Yu W and Wang Z 2025 Calibrating the simulated summer precipitation trend over the southern slope of the Tibetan Plateau in CMIP6 models using a sub-selection method *Adv. Clim. Change Res.* **16** 35–43
Pritchard H D 2019 Asia's shrinking glaciers protect large populations from drought stress *Nature* **569** 649–54
Wang L, Xu P, Chen W and Liu Y 2017a Interdecadal variations of the Silk Road pattern *J. Clim.* **30** 9915–32
Wang M, Huang Y, Franzke C L E, Yuan N, Fu Z and Boers N 2025 Evidence for preferred propagating terrestrial heatwave pathways due to Rossby wave activity *Nat. Commun.* **16** 4742
Wang Z, Duan A, Yang S and Ullah K 2017b Atmospheric moisture budget and its regulation on the variability of summer precipitation over the Tibetan Plateau *J. Geophys. Res.* **122** 614–30
Wang Z, Lei Y, Che H, Wu B and Zhang X 2024 Aerosol forcing regulating recent decadal change of summer water vapor budget over the Tibetan Plateau *Nat. Commun.* **15** 2233
Wang Z, Luo H and Yang S 2023 Different mechanisms for the extremely hot central-eastern China in July–August 2022 from a Eurasian large-scale circulation perspective *Environ. Res. Lett.* **18** 024023
Wang Z, Yang S, Luo H and Li J 2022 Drying tendency over the southern slope of the Tibetan Plateau in recent decades: role of a CGT-like atmospheric change *Clim. Dyn.* **59** 2801–13
Xie Y, Huang J, Wu G and Liu Y 2023 Potential vorticity dynamics explain how extratropical oceans and the Arctic modulate wintertime land-temperature variations *Earths Future* **11** e2022EF003275
Xie Y, Huang J, Wu G, Mi J, Liu Y, Su Z, Liu Y and Guan X 2025 Changing Northern hemisphere weather linked to warming amplification in high Mountain Asia *Commun. Earth Environ.* **6** 932
Yan H, Huang J, He Y, Liu Y, Wang T and Li J 2020 Atmospheric water vapor budget and its long-term trend over the Tibetan Plateau *J. Geophys. Res.* **125** e2020JD033297
Yang K, Wu H, Qin J, Lin C, Tang W and Chen Y 2014 Recent climate changes over the Tibetan Plateau and their impacts on energy and water cycle: a review *Glob. Planet. Change* **112** 79–91
Yao T *et al* 2012 Different glacier status with atmospheric circulations in Tibetan Plateau and surroundings *Nat. Clim. Change* **2** 663–7
Yao T D *et al* 2022 The imbalance of the Asian water tower *Nat. Rev. Earth Environ.* **3** 618–32
Zhang C, Tang Q and Chen D 2017a Recent changes in the moisture source of precipitation over the Tibetan Plateau *J. Clim.* **30** 1807–19
Zhang G *et al* 2017b Lake volume and groundwater storage variations in Tibetan Plateau's endorheic basin *Geophys. Res. Lett.* **44** 5550–60
Zhang Q, Shen Z, Pokhrel Y, Farinotti D, Singh V P, Xu C-Y, Wu W and Wang G 2023 Oceanic climate changes threaten the sustainability of Asia's water tower *Nature* **615** 87–93
Zhang W, Zhou T and Zhang L 2017c Wetting and greening Tibetan Plateau in early summer in recent decades *J. Geophys. Res.* **122** 5808–22
Zhao D, Zhang L and Zhou T 2022 Detectable anthropogenic forcing on the long-term changes of summer precipitation over the Tibetan Plateau *Clim. Dyn.* **59** 1939–52
Zhao Y, Xu C, Yu X, Liu Y and Ji X 2025 Atlantic oceanic droughts do not threaten Asian water tower *Nature* **638** E13–E15
Zhao Y and Zhou T 2021 Interannual variability of precipitation recycle ratio over the Tibetan Plateau *J. Geophys. Res.* **126** e2020JD033733
Zhou A, Yuan C, Luo J-J and Yamagata T 2024 Warming tropical Indian ocean wets the Tibetan Plateau *Geophys. Res. Lett.* **51** e2024GL108989
Zhou C, Zhao P and Chen J 2019 The interdecadal change of summer water vapor over the Tibetan Plateau and associated mechanisms *J. Clim.* **32** 4103–19